Experimental

Experimental

1: Aqueous solution (20 mL) containing $SrCl_2 \cdot 6H_2O$ (2.66 g, 10 mmol) and methylamine hydrochloride (1.36 g, 20 mmol) was added with $H_3[Co(CN)_6]$ (2.18 g, 10 mmol). The solution was stirred, filtered and evaporated to afford pale yellow block crystals of **1** (yield 78%, based on $H_3[Co(CN)_6]$). FT-IR (KBr): 3438, 2371, 2143, 1651, 1488, 1386, 925 cm^{-1}. Elemental analysis calcd (%) for $C_7H_{12}CoN_7O_3Sr$ (388.79): C 21.68, H 2.86, N 25.29. Found: C 21.91, H 2.27, N 25.54.

General measurements. Thermal gravimetric analysis (TGA) were carried out on a TA Instruments Q500. Powder X-ray diffraction (PXRD) was measured on a Rigaku SmartLab X-ray diffraction instrument at various temperatures. CHN elemental analysis was determined by the VARIO EL Ⅲ Elemental Analyzer. Solid-state ^2H NMR experiment of **1** at room temperature was performed on a Bruker Avance III HD 400WB (9.4 T) spectrometer with a commercial double resonance MAS probe at Larmor frequency of 61.29 MHz for ^2H. ^2H spectrum was recorded using a solid echo pulse sequence with a pulse spacing τ of 40 μs and pulse lengths of 5.0 μs for the 90 pulses. Recycle delays were set to 5 s and 16-step phase cycling was applied to suppress artifacts. The ^2H chemical shifts were determined using a solid external reference D_2O resonate at 4.7 ppm relative to tetramethylsilane.

Dielectric measurements. Crystalline-powdered samples were used for dielectric measurement in the form of discs. Silver conduction paste was used as electrodes. Multiple frequencies of dielectric measurement from 2 kHz to 1000 kHz of the sample was performed on a TongHui 2828 impedance analyzer of with an applied electric field of 0.5 V in the temperature range of 80−280 K. As to the HDS-LDS curves, in the first cycle, the sample of **1** was measured in the cooling run in the temperature range of 273−293 K to obtain the high dielectric states (HDS), then the heating run from 293 K to 423 K is needed to remove the H_2O molecules with the addition of silica gel into the sample chamber, and finally the sample was measured in the second cooling run from 298 K to about 90 K, through which the low dielectric states (LDS) were obtained. Other two cycles were followed by repeating the above process. For the second and the third cycle, the sample powder was pretreated through dehydration and rehydration to restore the state of the initial sample **1** before the measurements.

Adsorption–desorption measurements. Water vapor adsorption–desorption isotherms and adsorption kinetics were measured on a DVS Advantage-1 of Surface Measurement Systems using the powder sample **1**. The pretreatment procedure was carried out by first keeping the chamber RH% dropping from 25 to 0 in three steps with each step per 10 minutes. The temperature increased from 298 K to 423 K in 15 minutes and stayed at 423 K for 60 minutes before it dropped to 293 K again in 15 minutes and finally stayed at 298 K for 60 minutes. In the process of the isotherms

measurements, during the first run, RH% cycles from 0~95 in each step of 5% RH were employed and it was found that the powder began to dissolve after the RH% increases to 80% RH. So a second run was applied with the RH % cycles from 0 ~ 50 in each step of 2% RH (total two cycles). Equilibrium criteria: 0.01% weight percentage change per minute over 5 minutes and no longer than 120 minutes. In the adsorption kinetics measurements, the RH% stayed at setting RH% until equilibration and different RH% including 2%, 5%, 10%, 15%, 20%, 50% and 90% were recorded. Equilibrium criteria: 0.0005% weight percentage change per minute over 5 minutes and no longer than 720 minutes.

X-ray diffraction experiments. Variable-temperature single-crystal diffraction data of **1** and **2** were collected on a Rigaku Saturn 724^+ diffractometer equipped with Rigaku low-temperature gas spray cooler device by using Mo-Kα (λ = 0.71075 Å) radiation from a graphite monochromator. Before the measurement of **2**, in situ heating at 423 K was performed on the crystal **1** to remove the water and turn it into **2**. Data processing including empirical absorption correction was performed using the CrystalClear software package. The structures were solved by direct methods and successive Fourier synthesis and then refined by full-matrix least-squares refinements on F^2 using the SHELXTL software package. All non-hydrogen atoms were refined anisotropically. The hydrogen atoms of H_2O and methylammonium cation were generated geometrically. For the structure of **2**, the C and N atom of the disordered methylammonium cation were indistinguishable and refined as N atoms and no hydrogen atoms were added. Summary of crystallographic data, selected bond lengths and bond angles and details of hydrogen bonding interactions are given in Tables S1-S3.
CCDC 1518662 and 1518663 for **1** and 1518660 for **2** contain the supplementary crystallographic data for this paper. These data can be obtained free of charge from The Cambridge Crystallographic Data Centre via www.ccdc.cam.ac.uk/data_request/cif.

Theoretical calculations. Density functional theory (DFT) calculations were performed by using the Vienna ab initio simulation package (VASP).[1] The van der Waals interactions were included using the dispersion corrected semi-empirical DFT-D2 Grimme's method.[2] A single Γ-point calculation was sufficient for sampling the Brillouin zone.
References:

1 (a) Kresse, G.; Hafner, J. *Phys. Rev. B*, **1993**, *48*, 13115. (b) Kresse, G.; Furthmüller, J. *Phys. Rev. B* **1996**, *54*, 11169.
2 Grimme, S. *J. Comput. Chem.* **2006**, *27*, 1787.

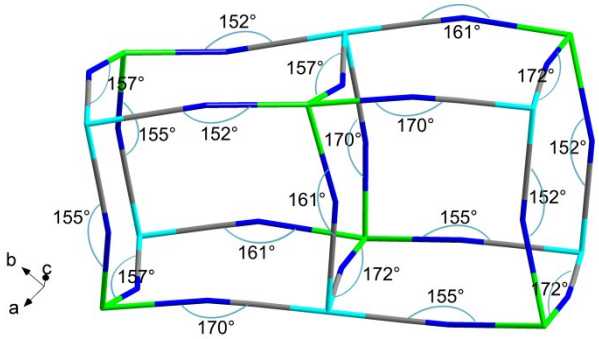

Figure S1. Bond angles of Sr–N–Co in the two different neighboring cages in **1** at 293 K.

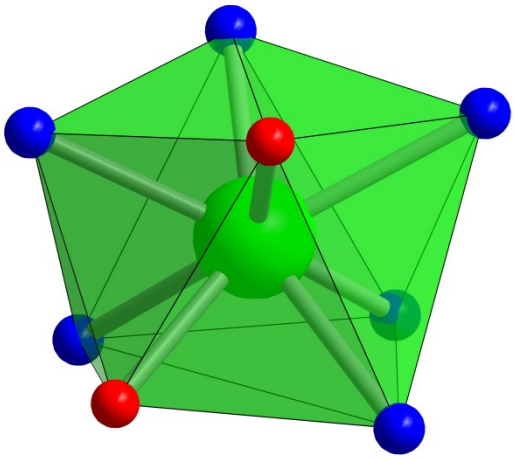

Figure S2. Coordination geometry of SrN_6O_2 in **1**. Green: Sr; blue: N; red: O.

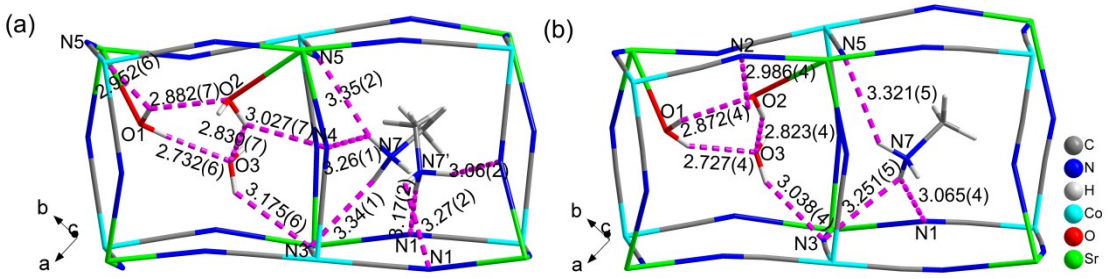

Figure S3. Hydrogen bonds between the guests and the host cages in **1** at (a) 293 K and (b) 93 K. Roseate dotted lines represent hydrogen bonds. The distance unit is Å.

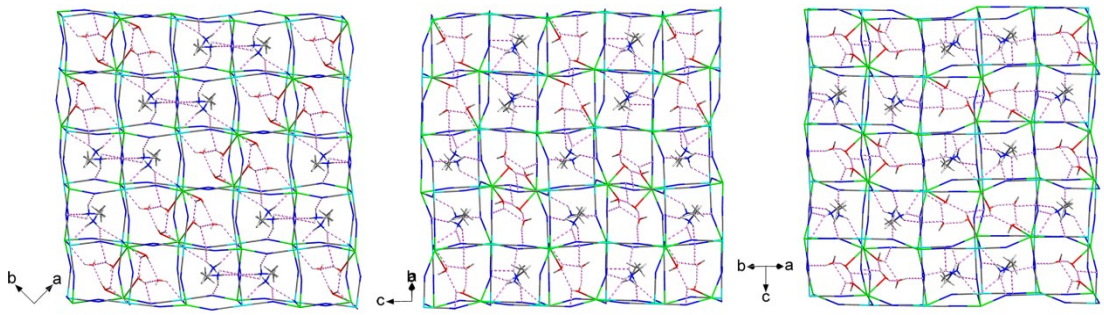

Figure S4. Packing diagrams of the host-guest frameworks of **1** at 293 K, shown in three directions.

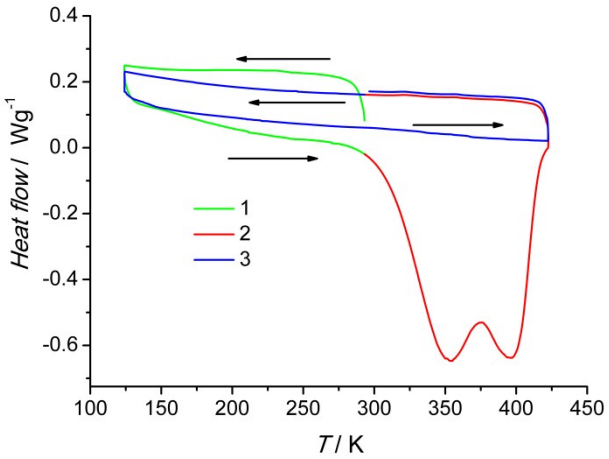

Figure S5. DSC curves of **1**.

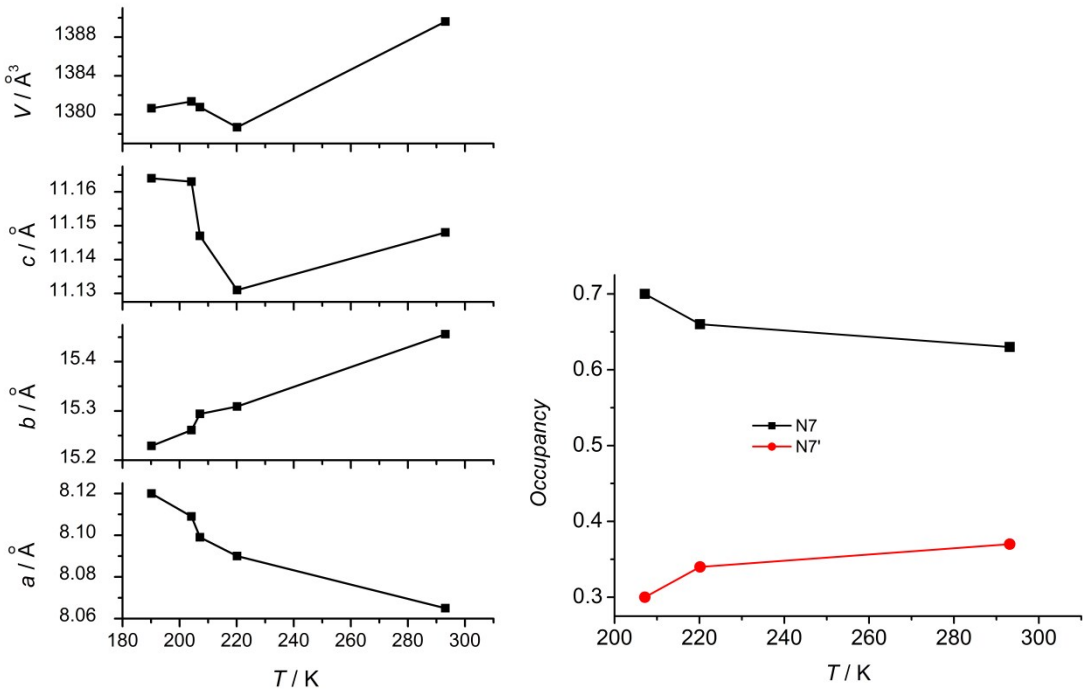

Figure S6. (left) Temperature dependence of the variable-temperature lattice parameters of **1**; (right) Temperature dependence of site occupancies of the disordered N atom of the MA cation.

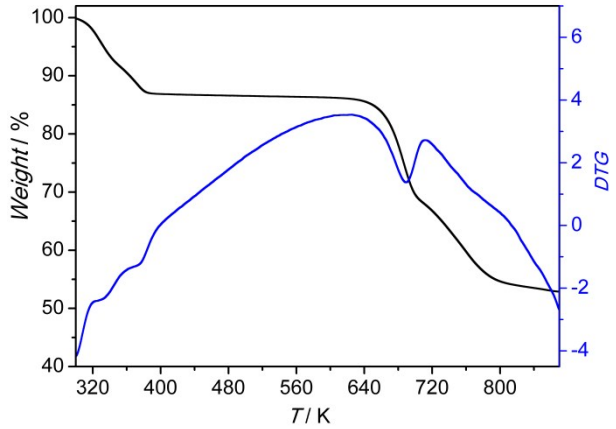

Figure S7. TGA curve of **1**.

A continuous weight loss of 13.2% (calc. 13.8%) is recorded between 300−400 K, corresponding to three water molecules per $(MA)(H_2O)[Sr(H_2O)_2Co(CN)_6]$.

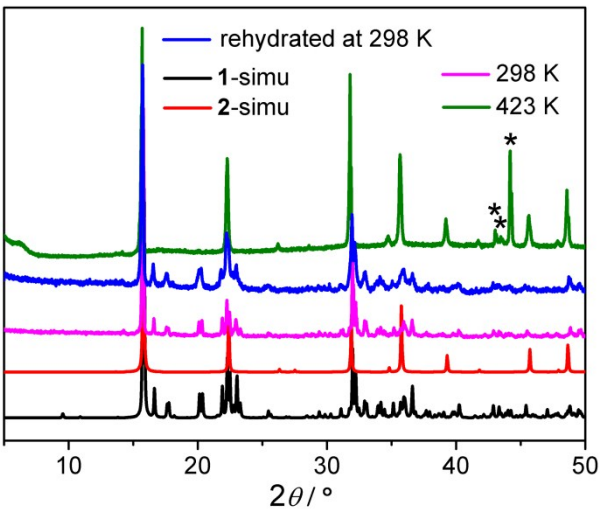

Figure S8. Variable-temperature PXRD patterns of **1** upon heating at 423 K and rehydration at 298 K, together with the simulated patterns of **1** and **2** from single-crystal X-ray diffraction data. The asterisked peaks arise from the sample holder.

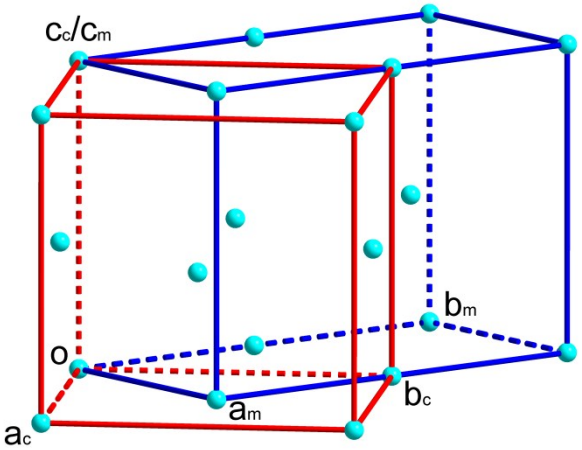

Figure S9. Orientation relationship between the phases of **1** (m = monoclinic phase; blue line) and **2** at 293 K (c = cubic phase; red line). The origin of the cell of **1** is shifted to the Co(III) center for a convenient comparison with the one of **2**. Only the Co(III) ions are shown for clarity.

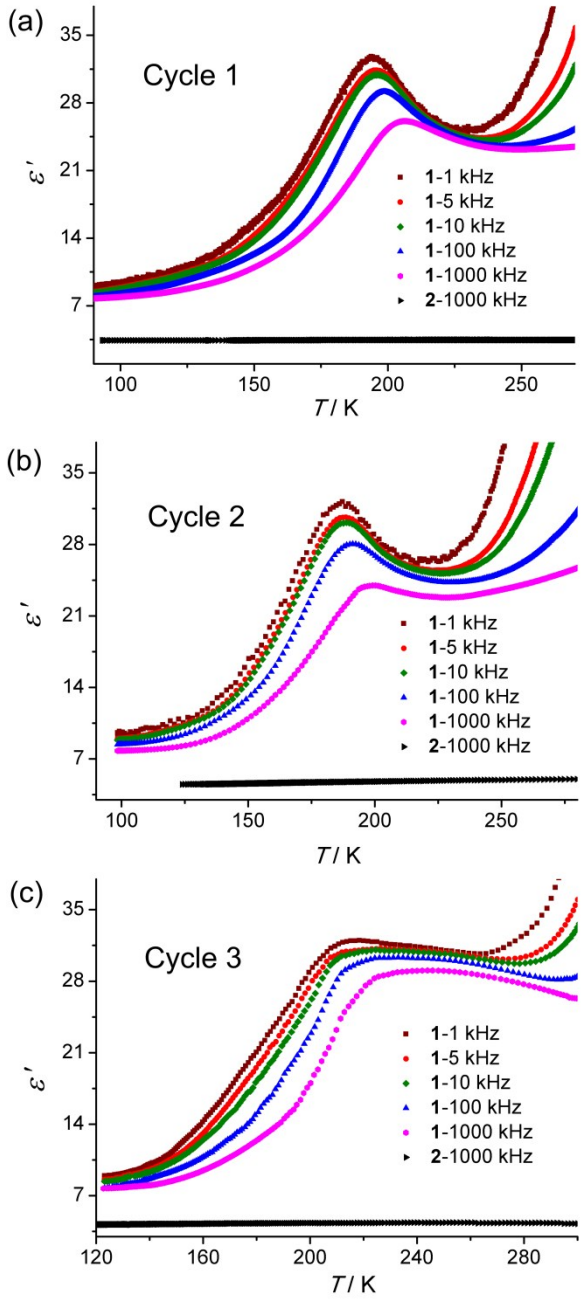

Figure S10. Temperature dependence of the real part of the dielectric constant of **1** and **2** in three consequential cycles upon dehydration and rehydration.

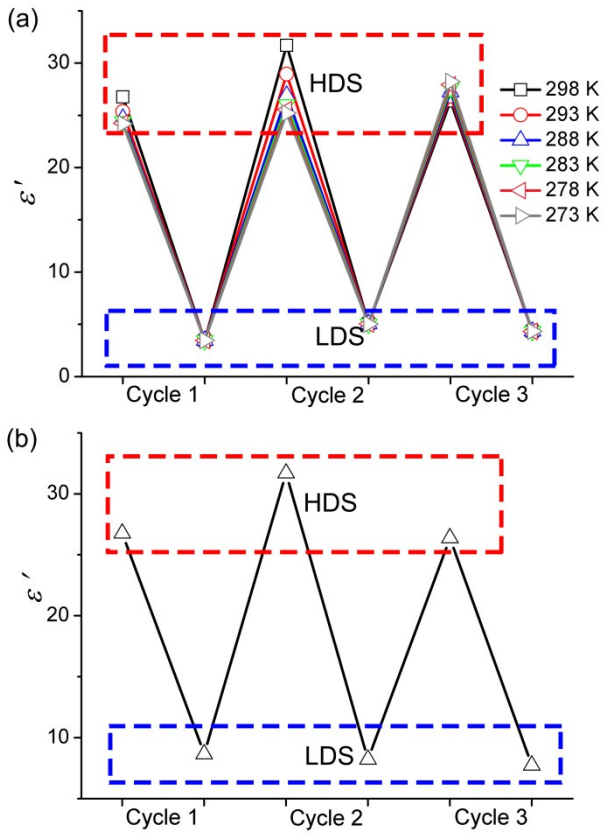

Figure S11. (a) Chemo-switching of the real part of the dielectric constant from **1** to **2** between HDS and LDS and (b) thermo-switching of the real part of the dielectric constant of **1** between HDS and LDS with the variation of temperature (HDS: 298 K, LDS: 123 K) in three consequential cycles upon dehydration and rehydration.

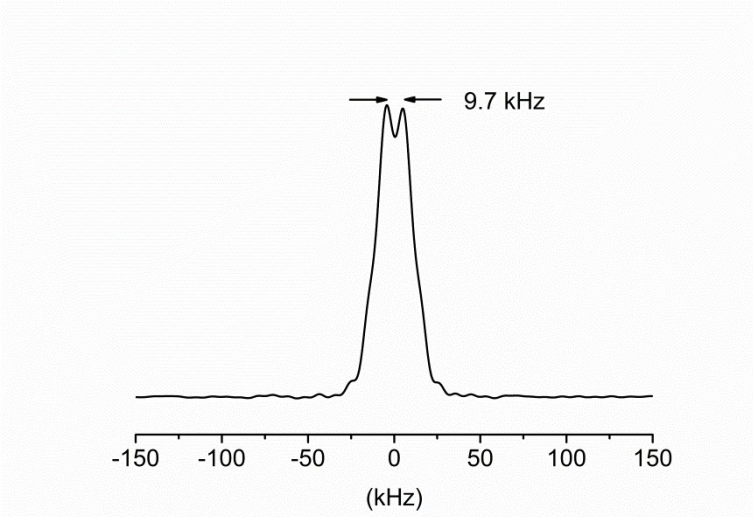

Figure S12. ^{2}H static NMR spectrum of **1** at 293 K with a quadrupolar splitting of 9.7 kHz.

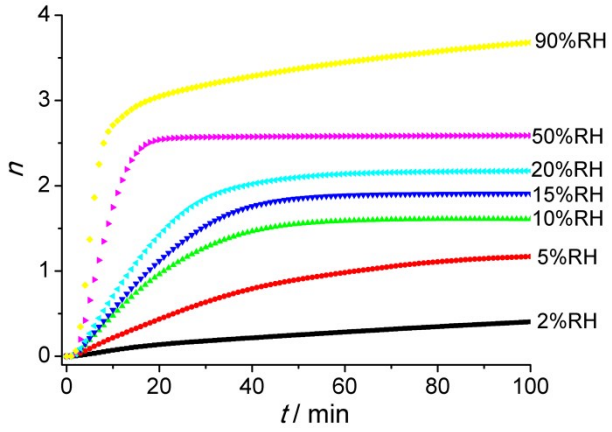

Figure S13. Kinetic study of the transition of **2**→**1** under different relative humidities. The n denotes the number of adsorbed water molecules per Sr ion

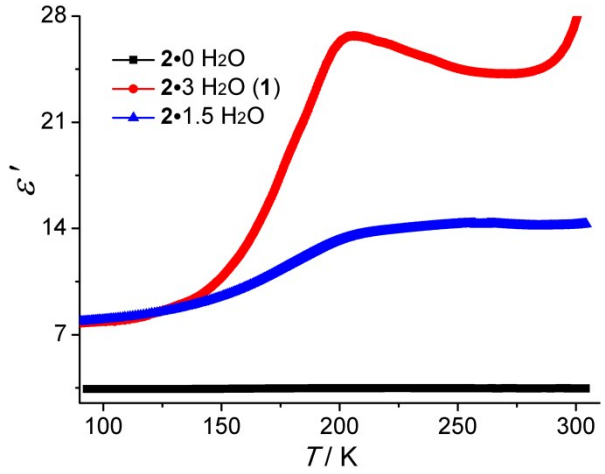

Figure S14. Temperature dependence of the real part of the dielectric constant of **2**·nH_2O on the water content at 1000 kHz.

Table S1. Crystallographic data and structural refinement details for **1** and **2**.

	1 (293 K)	**1** (93 K)	**2** (293 K)
Formula	$C_7H_{12}CoN_7O_3Sr$	$C_7H_{12}CoN_7O_3Sr$	$C_7H_6CoN_7Sr$
Formula weight	388.79	388.79	334.72
Crystal size / mm	0.20×0.20×0.20	0.20×0.20×0.20	0.20×0.20×0.20
Crystal system	monoclinic	monoclinic	cubic
Space group	$P2_1/n$	$P2_1/n$	$Fm\bar{3}m$
a / Å	7.716(2)	7.877(6)	11.217(4)
b / Å	16.218(3)	15.693(15)	11.217(4)
c / Å	11.266(2)	11.200(9)	11.217(4)
α / °	90	90	90
β /°	90.72(3)	91.77(2)	90
γ /°	90	90	90
V / Å^3	1409.6(5)	1384(2)	1411.4(14)
Z	4	4	4
D_{calc} / g·cm^{-3}	1.832	1.866	1.575
μ / mm^{-1}	4.975	5.067	4.940
F(000)	768	768	648
θ range / °	3.095−27.461	2.235−27.482	3.146−27.470
Reflns collected	9621	9960	2550
Independent reflns (R_{int})	3212 (0.0413)	3138 (0.0318)	113 (0.0343)
no. parameters	179	174	12
R_1[a], wR_2[b] [$I>2\sigma(I)$]	0.0440, 0.0852	0.0303, 0.0666	0.0139, 0.0335
R_1, wR_2 [all data]	0.0616, 0.0900	0. 0369, 0.0705	0.0139, 0.0335
GOF	1.176	1.075	1.242
$\Delta\rho$[c] / e·Å^{-3}	1.113, −0.799	0.694, −0.684	0.160, −0.130

[a] $R_1 = \Sigma||F_o| - |F_c||/\Sigma|F_o|$. [b] $wR_2 = [\Sigma w(F_o^2 - F_c^2)^2/\Sigma w(F_o^2]^2]^{1/2}$. [c] Maximum and minimum residual electron density.

Table S2. Bond lengths (Å) and bond angles (°) for **1** and **2**.

1 (293 K)			
Sr(1)−N(1)	2.727(4)	Sr(1)−N(1)−C(1)	155.1(4)
Sr(1)−N(2)	2.730(4)	Sr(1)−N(2)−C(2)#2	152.2(4)
Sr(1)−N(3)	2.716(4)	Sr(1)−N(3)−C(3)#3	172.6(4)
Sr(1)−N(4)	2.718(4)	Sr(1)−N(4)−C(4)#4	161.2(4)
Sr(1)−N(5)#1	2.694(4)	Sr(1)#5−N(5)−C(5)	156.6(4)
Sr(1)−N(6)	2.660(4)	Sr(1)−N(6)−C(6)	170.1(4)
Sr(1)−O(1)	2.608(4)	O(1)−Sr(1)−O(2)	83.07(17)
Sr(1)−O(2)	2.632(5)	O(1)−Sr(1)−N(1)	68.89(14)
		O(2)−Sr(1)−N(2)	66.12(16)
		N(1)−Sr(1)−N(2)	78.93(14)
		N(1)−Sr(1)−N(3)	75.76(13)

		N(1)−Sr(1)−N(4)	149.20(14)
		N(1)−Sr(1)−N(5)#1	121.36(15)
		N(1)−Sr(1)−N(6)	79.60(13)

Symmetry codes: #1 x−1/2, −y+1/2, z−1/2; # 2 −x+1/2, y+1/2, −z+1/2; #3 x−1/2, −y+1/2, z+1/2; #4 x−1, y, z; #5 x+1/2, −y+1/2, z+1/2.

1 (93K)

Sr(1)−N(1)	2.733(3)	Sr(1)−N(1)−C(1)	148.6(2)
Sr(1)−N(2)	2.722(3)	Sr(1)−N(2)−C(2)#2	150.8(3)
Sr(1)−N(3)	2.685(3)	Sr(1)−N(3)−C(3)#3	169.4(2)
Sr(1)−N(4)	2.693(3)	Sr(1)−N(4)−C(4)#4	160.4(2)
Sr(1)#1−N(5)	2.697(3)	Sr(1)#6 1−N(5)−C(5)	154.6(3)
Sr(1)−N(6)	2.644(3)	Sr(1)−N(6)−C(6)	168.6(2)
Sr(1)−O(1)	2.614(3)	O(1)−Sr(1)−O(2)	79.90(9)
Sr(1)−O(2)	2.618(3)	O(1)−Sr(1)−N(1)	71.59(9)
		O(2)−Sr(1)−N(1)	139.28(9)
		N(1)−Sr(1)−N(2)	80.01(10)
		N(1)−Sr(1)−N(3)	74.43(8)
		N(1)−Sr(1)−N(4)	146.93(8)
		N(1)−Sr(1)−N(5)#5	122.95(9)
		N(1)−Sr(1)−N(6)	75.31(10)

Symmetry codes: #1 x+1/2, −y+1/2, z+1/2; # 2 −x+1/2, y+1/2, −z+1/2; #3 x−1/2, −y+1/2, z−1/2; #4 x−1, y, z; #5 x−1/2, −y+1/2, z−1/2

2 (293 K)

Sr(1)−N(1)	2.583(3)	C(1)#2−Co(1)−C(1)#3	180.0
Co(1)−C(1)	1.890(3)	C(1)#2−Co(1)−C(1)#4	90.0
C(1)−N(1)	1.136(4)	N(1)−Sr(1)−N(1)#5	90.0
N(2)−N(2)#1	1.4567	N(1)−Sr(1)−N(1)#6	180.0
		N(1)−C(1)−Co(1)	180.0
		C(1)−N(1)−Sr(1)	180.0

Symmetry codes: #1 −x+1/2, y, −z+1/2; #2 −y+1, −z+1/2, −x+1/2; #3 y, z+1/2, x−1/2; #4 −x+1, −y+1, −z; #5 −y+3/2, −z+1, −x+1/2; #6 −x+1, −y+2, −z.

Table S3. Hydrogen bonds (Å, °) for **1**.

D−H···A	D−H	H···A	D···A	D−H···A
1 (293 K)				
N7'−H7'A···N1 [x−1/2, −y+1/2, z+1/2]	0.90	2.27	3.17(2)	175.6
N7'−H7'B···N1 [−x+1/2, y−1/2, −z+3/2]	0.90	2.67	3.27(2)	125.4
N7'−H7'C···N2 [−x+1/2, y−1/2, −z+3/2]	0.90	2.38	3.06(2)	132.8

N7−H7A···N3 [x−1/2, −y+1/2, z+1/2]	0.90	2.51	3.34(1)	154.4
N7−H7B···N5 [x−1/2, −y+1/2, z+1/2]	0.90	2.52	3.35(2)	153.5
N7−H7B···N4 [x, y, z+1]	0.90	2.65	3.26(1)	125.7
O1−H1B···O3	0.85	1.91	2.732(6)	161.1
O1−H1A···N5 [x−1/2, −y+1/2, z−1/2]	0.85	2.55	2.952(6)	110.4
O1−H1A···O2 [−x, −y+1, −z]	0.85	2.28	2.882(7)	127.8
O2−H2B···N4	0.85	2.47	3.027(7)	123.5
O2−H2B···O3 [−x, −y+1, −z]	0.85	2.31	2.830(7)	120.3
O3−H3A···N3 [−x+1/2, y+1/2, −z+1/2]	0.85	2.54	3.175(6)	132.1
1 (93 K)				
N7−H7B···N3 [x−1/2, −y+1/2, z+1/2]	0.89	2.67	3.251(5)	123.6
N7−H7B···N1 [x−1/2, −y+1/2, z+1/2]	0.89	2.25	3.065(4)	151.5
N7−H7C···N5 [x−1/2, −y+1/2, z+1/2]	0.89	2.57	3.321(5)	142.2
O1−H1A···O2 [−x, −y−1/2, −z]	0.85	2.17	2.872(4)	140.4
O1−H1B···O3	0.85	1.96	2.727(4)	150.1
O2−H2A···N2	0.85	2.43	2.986(4)	123.5
O2−H2B···O3 [−x, −y+1, −z]	0.85	2.04	2.823(4)	153.9
O3−H3A···N3 [−x+1/2, y+1/2, −z+1/2]	0.85	2.29	3.038(4)	147.6